Extended x-ray-absorption fine-structure study of copper under high pressure

J. Freund and R. Ingalls
Department of Physics (FM-15), University of Washington, Seattle, Washington 98195

E. D. Crozier
Department of Physics, Simon Fraser University, Burnaby, British Columbia, Canada V5A 1S6
(Received 16 December 1988)

We examine copper as a pressure calibrant for extended x-ray-absorption fine-structure (EXAFS) measurements of solids under pressures ranging from 0 to 10 GPa. Great care must be exercised both in the theoretical formulation of EXAFS and in the data analysis in order to achieve the high precision required to make copper a useful pressure marker. From the first-shell k-space data, phase and amplitude information is extracted both with the ratio method and from fitting parameters with the help of theoretically calculated central-atom phase shifts [B.-K. Teo and P. A. Lee, J. Am. Chem. Soc. **101**, 2815 (1979)] and curved-wave backscattering phase shifts and amplitudes [A. G. McKale *et al.*, J. Am. Chem. Soc. **110**, 3763 (1988)]. Both techniques yield practically identical results confirming the reliability of the phase and amplitude tabulations. But both techniques suffer from the ambiguity that the results depend on how many EXAFS parameters are kept variable. It is shown that, for copper, only nearest-neighbor distances and second cumulants (EXAFS Debye-Waller factors) have to be taken into account. Then pressures can be determined with an accuracy of about 0.5 GPa. We also present two models for the pressure dependence of the second cumulant: (1) a correlated Debye model along with simple parametrizations of the isothermal equation of state and the Grüneisen parameter, and (2) a model for the calculation of the moments of the nearest-neighbor distance distribution from an expansion to third order of the potential energy. Both models confirm our data analysis.

I. INTRODUCTION

Extended x-ray-absorption fine structure (EXAFS) has been proven to be a valuable tool in various branches of solid-state physics, but few attempts have so far been made to use it in high-pressure physics. High-pressure EXAFS is limited by the diamond anvils commonly used to compress materials because at certain x-ray energies Bragg reflections suddenly reduce the transmitted intensity, giving rise to spurious absorption peaks which cannot satisfactorily be separated from the EXAFS.[1,2] For this reason we replaced diamond by boron carbide (B_4C) anvils which are polycrystalline but not transparent for visible light. In so doing we precluded use of the state-of-the-art ruby-fluorescence pressure-calibration technique. A new pressure maker was thus called for.

The most natural way of determining pressure in our experiments is from the EXAFS itself by mixing with our sample a material whose isothermal equation of state is well known and whose compressibility is large. Also, its EXAFS must be easy to measure (atomic numbers neither too low nor too high), must not interfere with the EXAFS of the sample under investigation and must have easily separable (in **r** space) first- and second-nearest-neighbor shells. Some of the alkali halides fulfill all of these criteria and have been found useful in our experiments.[3–5] A detailed report on the EXAFS of alkali halides under pressure will be written later. In this paper we examine the canonical EXAFS substance, copper, as a pressure marker. Even though it is relatively incompressible it has the advantage of being one of the best understood materials.

After a short section on our experimental setup, the EXAFS formula including third and fourth cumulants is derived from a thermal average of the basic EXAFS function $\chi(k)$. The two standard data-analysis techniques are then introduced: the ratio method and the fitting of parameters with help of theoretically calculated EXAFS phases and amplitudes. These techniques are required to estimate the errors incurred in the reduction of the absorption spectrum to a first-shell **k**-space data set. Single-shell data thus produced are then subjected to the ratio and the parameter-fitting routines which are intrinsically ambiguous because the results depend on the number of parameters considered variable. A careful analysis of the differing results eliminates all but one method: The pressure-induced phase change may be considered to depend *only* on the nearest-neighbor distance, while the amplitude change depends *only* on the second cumulant (EXAFS Debye-Waller factor). This result must not be generalized to other substances. But it shows the particular usefulness of copper as a pressure calibrant in EXAFS studies. When the data analysis is thus done with the greatest care, it becomes clear that pressure-induced *changes* in nearest-neighbor distances can be calculated with an accuracy of 0.002 to 0.003 Å, thus yielding pressures with an accuracy of about 0.5 GPa. Finally, we present two theoretical calculations. The first one uses Rehr's correlated Debye model to predict the second cumulant as a function of pressure. The second one starts

from first principles and, with minor simplifying approximations, predicts the pressure dependence of the first and second moments and therefore the first and second cumulants, as well. Both calculations confirm our data analysis.

II. EXPERIMENTATION

The geometry of the high-pressure cell used in the experiments has been shown previously.[2] The sample consists of a fine powder of the material to be investigated and a copper foil of 0.005 mm thickness, all embedded in soft epoxy which acts as a pressure medium. The sample has a diameter of about 0.8 mm and a thickness of about 0.4 to 0.6 mm and is radially confirmed by an inconel gasket. Axially, the sample is sealed between two boron-carbide anvil tips with flats of 2.0 or 2.5 mm diam. In our axial cell geometry the x-ray beam passes through about 1 to 2 mm of boron carbide on each side of the sample. The boron-carbide anvils are held by hardened steel pistons which are moved by a hydraulic fluid which is under a pressure of typically 10 to 20 MPa before one boron-carbide anvil breaks and the high-pressure experiment is terminated. The highest pressures we can achieve are limited by the diameter and thickness of the boron-carbide anvils. A reduction of the diameter by a factor of R reduces the photon flux by a factor of R^2. Increasing the thickness of the anvils decreases the photon flux exponentially. With our present anvils we need an integration time of about one second for each monochromator position, i.e., we can obtain one EXAFS spectrum in about 15 min.

All experiments were performed at wiggler beamlines of the Stanford Synchrotron Radiation Laboratory (SSRL) as described in the literature.[7,8] All experiments were made in transmission mode. The most common errors in such an experiment are known as the thickness effect.[9,10] They include leakage of higher harmonics which we try to minimize by detuning the monochromator crystal. Since the detuning has to be done several times in the course of an experiment, two data sets are not always completely comparable, affecting the amplitude in particular. Another possibly serious error for the amplitude results from the finite width of the energy band that passes through the sample, or rather from the variation of this band width by means of the slits.[11] Errors due to pinholes and radiation leaking around the sample are minimized by use of homogeneous samples (foils) together with a collimator of diameter 0.66 mm.

The copper data were obtained in eight different experiments over a span of five years. In all experiments we usually took two or three EXAFS spectra at zero pressure and at each higher pressure. Therefore, we have four or nine partially independent pairs of data sets for each pressure, which allows us to plot error bars for each individual data point.

III. CUMULANT EXPANSION

When only single-scattering processes are considered, which is no limitation in nearest-neighbor analyses, the EXAFS formula for K-shell absorption is given by

$$\chi(k)=-\sum_j \frac{N_j F_j(k,\pi)}{k} \times \mathrm{Im}\left[\left\langle \frac{1}{r_j^2} e^{-2r_j/\lambda} e^{2ikr_j}\right\rangle e^{i\Phi_j(k)}\right], \quad (1)$$

where the summation is over the shells, k is the photoelectron wave number, N_j the coordination number, $F_j(k,\pi)$ the backscattering amplitude, and r_j the momentary position of an atom (not to be confused with its average position R_j) of shell j. $\Phi_j(k)$ is the combined central-atom and backscattering-atom phase function of that shell. The parameter λ, usually denoted as mean-free path, is meant to include all many-body effects which have not already been included in the backscattering amplitude. In the literature,[12] the mean-free path is taken to be k dependent, with a wide minimum in the central region of a typical EXAFS spectrum. Since the k dependence is rather weak and would require the introduction of two new parameters, we choose to keep λ constant in all data analyses. But it must be borne in mind that, unavoidable as it may be, the neglect of this k dependence limits the accuracy of all amplitude-dependent parameters.

The angular brackets $\langle\ \rangle$ in Eq. (1) denote a thermal average. This averaging produces the cumulant expansion which is central to our study. Since there are only brief derivations of this expression in the literature,[13,14] we produce it more fully here. The *definition* of cumulants $\sigma^{(1)},\sigma^{(2)},\ldots,\sigma^{(n)},\ldots$ is given by [15]

$$\exp\left[\sigma^{(1)}t+\frac{\sigma^{(2)}t^2}{2!}+\cdots+\frac{\sigma^{(n)}t^n}{n!}+\cdots\right] = 1+\mu_1 t+\frac{\mu_2 t^2}{2!}+\cdots+\frac{\mu_n t^n}{n!}+\cdots, \quad (2)$$

where μ_n denotes the nth moment of a distribution. The first four cumulants, expressed in terms of moments, can be obtained by taking the logarithm of (2), expanding the right-hand side and comparing terms of like powers in t:

$$\sigma^{(1)}=\mu_1, \quad (3a)$$

$$\sigma^{(2)}=\mu_2-\mu_1^2, \quad (3b)$$

$$\sigma^{(3)}=\mu_3-3\mu_2\mu_1+2\mu_1^3, \quad (3c)$$

$$\sigma^{(4)}=\mu_4-4\mu_3\mu_1-3\mu_2^2+12\mu_2\mu_1^2-6\mu_1^4. \quad (3d)$$

Replacing t by $2ik$, one can then write

$$\exp\left[\sum_{n=1}^{\infty}\frac{\sigma_j^{(n)}(2ik)^n}{n!}\right]=\langle e^{2ikr_j}\rangle \quad (4)$$

as can easily be verified by expanding the right-hand side of (4). Noting that $\sigma_j^{(1)}=R_j$ and $\sigma_j^{(2)}=\sigma_j^2$, the EXAFS

Debye-Waller factor, one writes

$$\langle e^{2ikr_j}\rangle = \exp\left[2ikR_j - 2\sigma_j^2k^2 - \frac{4i}{3}\sigma_j^{(3)}k^3 + \tfrac{2}{3}\sigma_j^{(4)}k^4 - \cdots\right]. \quad (5)$$

Introducing x_j as a deviation from the mean, $x_j = r_j - R_j$, the bracket in (1) is written as

$$\frac{1}{R_j^2}e^{-2R_j/\lambda}e^{2ikR_j}\left\langle \frac{1}{(1+x_j/R_j)^2}e^{-2x_j/\lambda}e^{2ikx_j}\right\rangle$$

which gives, after Taylor expansion to second order in x_j,

$$\frac{1}{R_j^2}e^{-2R_j/\lambda}e^{2ikR_j}\left[\langle e^{2ikx_j}\rangle - \left[\frac{2}{\lambda}+\frac{2}{R_j}\right]\frac{1}{2i}\frac{d}{dk}\langle e^{2ikx_j}\rangle + \left[\frac{2}{\lambda^2}+\frac{4}{R_j\lambda}+\frac{3}{R_j^2}\right]\frac{1}{(2i)^2}\frac{d^2}{dk^2}\langle e^{2ikx_j}\rangle\cdots\right].$$

Upon noting that $\langle e^{2ikx_j}\rangle = \langle e^{2ikr_j}\rangle e^{-2ikR_j}$ and inserting (5) into the above expression one obtains a lengthy sum one term of which is about one order of magnitude larger than all others. Neglecting the small terms yields

$$\frac{1}{R_j^2}\exp(-2R_j/\lambda)\exp(2ikR_j)\exp\left[-2\sigma_j^2k^2 - \frac{4i}{3}\sigma_j^{(3)}k^3 + \tfrac{2}{3}\sigma_j^{(4)}k^4\right]\left[1 - i\left[\frac{1}{\lambda}+\frac{1}{R_j}\right]4\sigma_j^2k\right].$$

Since the imaginary part is small the bracketed term can approximately be rewritten as

$$\exp\left[-\frac{4i\sigma_j^2k}{R_j}\left[1+\frac{R_j}{\lambda}\right]\right].$$

Finally, the EXAFS formula including second-order corrections, i.e., third and fourth cumulants, becomes

$$\chi(k) = -\sum_j A_j(k)\sin[\Psi_j(k)] \quad (6a)$$

with the amplitude

$$A_j(k) = \frac{N_jF_j(k,\pi)}{kR_j^2} \times \exp(-2R_j/\lambda)\exp(-2\sigma_j^2k^2 + \tfrac{2}{3}\sigma_j^{(4)}k^4) \quad (6b)$$

and the phase

$$\Psi_j(k) = 2k\left[R_j - \frac{2\sigma_j^2}{R_j}\left[1+\frac{R_j}{\lambda}\right]\right] - \tfrac{4}{3}\sigma_j^{(3)}k^3 + \Phi_j(k)\,. \quad (6c)$$

Henceforth we deal only with single shells, therefore $j=1$ and the summation symbol as well as the subscript j are omitted.

IV. RATIO METHOD AND PARAMETER FITTING

The most straightforward data-analysis technique is the ratio method invented by Stern *et al.*[16] It was extended to include higher cumulants by Bunker[17] and Tranquada,[5,8,13] but it has never been presented with all terms, including energy shift.

The ratio method starts with the decomposition of the single shell $\chi(k)$ [whose preparation from a multishell $\chi(k)$ is explained in the next section] into phase and amplitude by means of two successive Fourier transforms.[18] In dealing with two data sets at different pressures, it must not be assumed *a priori* that the wave vectors k are the same for both sets, 1 and 2, since the zero of the kinetic energy of the photoelectron might shift with increasing pressure. Therefore one writes

$$k_1 = \left[k_2^2 - \frac{\Delta E}{3.81}\right]^{1/2} \approx k_2 - \frac{\Delta E}{7.62k_2}\,. \quad (7)$$

where the subscripts denote the data sets and ΔE is the energy shift between the two sets in eV. The unit of k is Å^{-1}. Neglecting higher-order terms, the difference between the phases of the two sets, $\Delta\Psi(k_2) = \Psi_1(k_2) - \Psi_2(k_2)$, is then given by

$$\Delta\Psi(k) = -\frac{\Delta E}{3.81}\left[R_1 - \frac{2\sigma_1^2}{R_1}\left[1+\frac{R_1}{\lambda_1}\right]\right]\frac{1}{k} + 2\left[\Delta R - 2\left[\frac{\sigma_1^2}{R_1} - \frac{\sigma_1^2-\Delta\sigma^2}{R_1-\Delta R} + \frac{\sigma_1^2}{\lambda_1} - \frac{\sigma_1^2-\Delta\sigma^2}{\lambda_1-\Delta\lambda}\right]\right]k - \tfrac{4}{3}\Delta\sigma^{(3)}k^3 \quad (8)$$

with $k=k_2$, $\Delta R = R_1 - R_2$, etc. It assumes that $\Phi_1(k) = \Phi_2(k)$ which gives an error of about 15% in ΔE. Even for $\Delta E = 0$ this assumption is not evident and will be examined in Sec. VI. When a least-squares fit of the form $a_{-1}k^{-1} + a_1k^1 + a_3k^3$ is made, the three unknown parameters ΔE, ΔR, and $\Delta\sigma^{(3)}$ can be obtained provided the parameters with subscript 1 are known and the Δ terms in the right half of the second term are initially set to zero.

In a similar way, the logarithm of the ratio of the amplitudes of two sets 1 and 2 is given by

$$\ln\left[\frac{A_1(k)}{A_2(k)}\right] = \ln\left[\frac{N_1(R_1-\Delta R)^2}{(N_1-\Delta N)R_1^2}\right] - 2\left[\frac{R_1}{\lambda_1} - \frac{R_1-\Delta R}{\lambda_1-\Delta\lambda}\right] - 2\Delta\sigma^2k^2 + \tfrac{2}{3}\Delta\sigma^{(4)}k^4\,. \quad (9)$$

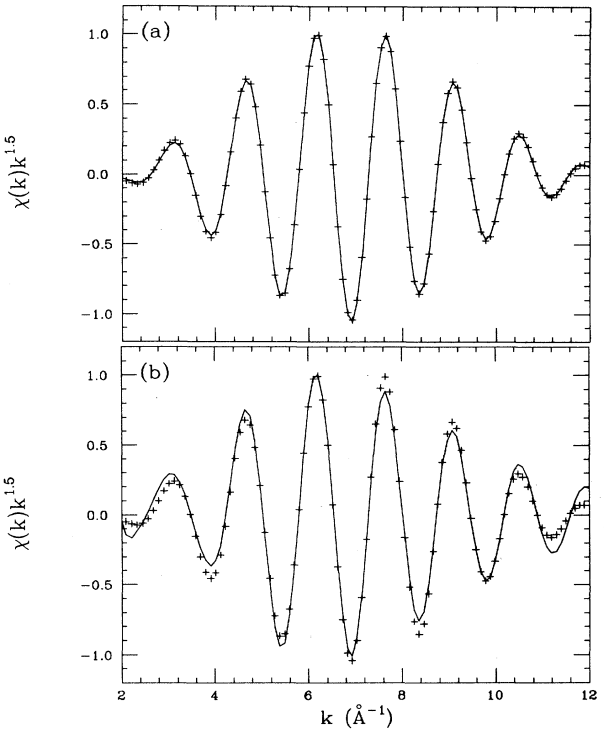

FIG. 1. Example of a parameter fit. ΔE, R, λ, and σ^2 were variable. The crosses are the data, the solid line is the fit. (a) The fit was subjected to forward and backward Fourier transforms; (b) no Fourier transforms were applied. The goodness-of-fit parameters are 4 and 175 (arbitrary units), respectively.

It assumes that $F_1(k,\pi)=F_2(k,\pi)$ which will also be examined in Sec. VI. A least-squares fit with a polynomial of the form $a_0+a_2k^2+a_4k^4$ is made to obtain ΔN (if N_1, λ_1, and $\Delta\lambda$ are known) or $\Delta\lambda$ (if N_1, ΔN, and λ_1 are known), $\Delta\sigma^2$, and $\Delta\sigma^{(4)}$.

While for copper at zero pressure and room temperature $N_1=12$ and $R_1=2.556$ Å are well known, σ_1^2 and λ_1 are not. Several theoretical and experimental investigations indicate that the former ranges between 7.3×10^{-3} and 9.2×10^{-3} Å^2 (Refs. 6 and 19–21), while the latter is about 7–8 Å.[16,22,23] Here we take $\sigma_1^2=7.7\times10^{-3}$ Å^2 and $\lambda_1=8$ Å. Fortunately enough, ΔE and ΔR in (8) and (9) depend very little on the input of σ_1^2 and λ_1, and except for the determination of ΔN and $\Delta\lambda$ no error is incurred.

It is obvious that an iterative procedure is required to solve for both phase and amplitude parameters, but the results converge very rapidly. It must also be mentioned that it is advisable to weight the fits with $[A_1A_2/(A_1+A_2)]^2$ in order to deemphasize the low-k and high-k regions which get distorted when the single-shell data sets are prepared, as will be shown in the next section.

The other major data-analysis technique is parameter fitting. It is based on the assumption that an EXAFS spectrum can be simulated perfectly well with theoretically calculated values for the central-atom and backscattering-atom phase shifts and the backscattering amplitude. Central-atom phase shifts, calculated with Herman-Skillman wave functions, were taken from Teo and Lee[24] and interpolated with the polynomial $a_0+a_1k+a_2k^2+a_{-3}k^{-3}$.[25] Backscattering-atom phase shifts and amplitudes were taken from McKale's[26–28] recent calculations that make use of the curved-wave formalism and therefore extend the EXAFS analysis down to lower k (about $k=2.0$ Å) than before.

In parameter fitting an EXAFS spectrum is calculated with a trial set of numbers for the unknown parameters, and the sum of the squares of the deviation between fit and data, the goodness-of-fit parameter, is calculated. This procedure is repeated with different choices of numbers until the goodness-of-fit parameter reaches a minimum. Since this technique is inefficient when the number of parameters is large the problem is split into fitting the phase parameters ΔE and R and amplitude parameters N (or λ) and σ^2 separately. $\sigma^{(3)}$ and $\sigma^{(4)}$ are kept fixed and each of the above-mentioned parameters may also be kept constant, if desired. The best fitting is achieved by setting up a grid of 3×3 numbers for the two phase parameters, calculating the nine goodness-of-fit parameters, selecting the smallest one, and continuing with a smaller grid. When stable results are achieved the procedure is repeated for the two amplitude parameters. Finally, a four-dimensional parameter space is spanned and a gradient search[29,30] is started which does not usually change the results of the grid searches very much. A notable improvement in the goodness-of-fit can be achieved when the fits are subjected to the same succession of Fourier forward- and backtransforms that are used to produce the single-shell data (see next section). Figure 1 shows that the improvement is particularly great at the low-k and high-k ends of the spectrum.

V. PREPARATION OF DATA SETS

A recent review article on data preparation and analysis has been written by Sayers and Bunker.[31] Data preparation of copper in particular has already been dealt with by Lengeler and Eisenberger[22] and Cook and Sayers.[32] It is desirable to go into greater detail here. Analysis starts with background removal which is fairly standardized: The arbitrary determination of the zero of the photoelectron kinetic energy (e.g., the little peak in the middle of the edge for copper) is followed by the preedge background removal with an appropriate fit and the postedge background removal with a cubic spline. Variation of the number of knots (typically four) and the weighting scheme (typically k^2) has little influence on the results. Ideally, the EXAFS should be obtained from

$$\chi(E)=\frac{\mu(E)-\mu_0(E)}{\mu_0(E)}\ , \tag{10}$$

where $\mu(E)$ and $\mu_0(E)$ are the actual absorption and the background absorption, respectively, after subtraction of the preedge background. But the preedge background cannot reliably be extrapolated far beyond the edge. In practice, therefore, one divides by $\mu_0(E_0)$ in (10) where E_0 is the edge position. This procedure poses another limitation to the accuracy of amplitude parameters.

TABLE I. Comparison between input and output of four EXAFS parameters: Δr, $\Delta\sigma^2$, $\Delta\sigma^{(3)}$, and $\Delta\sigma^{(4)}$. Goodness-of-fit parameters of phase-difference and amplitude-ratio fits in arbitrary units. Gaussian k window: 2.5–5.0 and 10.0–12.5 Å^{-1}, as described in the text, weighted with $k^{1.5}$. Square r window of low-pressure set: 1.75–2.64 Å, of high-pressure set as indicated, k range used for fitting; 4–10 Å^{-1}.

r-window (Å): (high pressure)		Δr (Å)	$\Delta\sigma^2$ (10^{-3} Å^2)	$\Delta\sigma^{(3)}$ (10^{-4} A^3)	$\Delta\sigma^{(4)}$ (10^{-5} Å^4)	Goodness-of-fit Phase	Amplitude
1.75–2.64	input	0.020	1.00	1.00	1.00	2483	95
	output	0.021	0.93	1.27	0.84		
1.72–2.64	input	0.020	1.00	1.00	1.00	705	79
	output	0.020	1.35	0.75	2.59		
1.75–2.61	input	0.020	1.00	1.00	1.00	425	45
	output	0.020	0.82	1.11	0.29		
1.72–2.61	input	0.020	1.00	1.00	1.00	3338	72
	output	0.019	1.23	0.59	2.04		
1.72–2.61	input	0.050	2.00	3.00	2.00	1160	193
	output	0.049	2.18	2.83	2.89		
1.69–2.61	input	0.050	2.00	3.00	2.00	2630	230
	output	0.049	2.55	2.44	4.50		
1.72–2.58	input	0.050	2.00	3.00	2.00	787	536
	output	0.048	2.08	2.58	2.47		
1.69–2.58	input	0.050	2.00	3.00	2.00	5560	396
	output	0.048	2.45	2.19	4.08		

The next step in data analysis, the two Fourier transforms from **k** space to **r** space and back into **k** space, are potentially dangerous because of the well-known truncation effects. This is especially true for the backtransform. In order to minimize transform artifacts EXAFS spectra are simulated with the tabulated values for the phases and amplitudes and subjected to the transform routines and to the ratio- or parameter-fitting routines. Then the difference between input and output determines the quality of the transforms.

The best **k**-space window and weighting scheme can be found with an artificial spectrum consisting of only one shell because then a very large **r**-space window can be taken such that the backtransform does not affect the results. It is found that moderate smoothing at the low-k and the high-k end (e.g., a Gaussian with 10% at $k=2.5$ Å^{-1}, 100% from $k=5.0$ Å^{-1} to $k=10.0$ Å^{-1}, and 10% at $k=12.5$ A^{-1}) does a better job than a boxcar window. Weighting with k^0 or $k^{1.5}$ does not make a difference, except that in the former case the transform in **r** space is a little wider. The same result holds for larger exponents. In anticipation of the problems with the backtransform it is highly preferable to have the narrowest possible **r**-space transform, and therefore one chooses a $k^{1.5}$ weighting.

By gradually decreasing the width of the **r**-space window the fits become worse and the output starts to deviate from the input, especially for the sensitive higher cumulants. When artificial EXAFS sets consisting of several shells are used, some further deterioration cannot be avoided because the first and second shells partially overlap. When artificial EXAFS data are finally replaced with real data one is even forced to truncate the low-r side lobe because that portion of the spectrum is contaminated with low-frequency background artifacts. It seems that the best window is a boxcar from about 1.72 Å to about 2.64 Å at $p=0$. For higher pressures the window has to be moved to smaller values. Even though the goodness-of-fit depends considerably on small variations of the **r** windows, the results are relatively stable, as demonstrated in Table I. In particular, the change in nearest-neighbor distance can be determined within about ±0.001 Å, the changes in second, third, and fourth cumulants can be calculated with accuracies of about 20%, 20% and 100%, respectively. We can therefore expect useful results, except for the fourth cumulant.

VI. RESULTS

In (8) and (9) the phase differences and amplitude ratios are fitted with three parameters each. It is not always advisable to do so because the parameters are strongly correlated and, even though the goodness-of-fit parameter decreases, the parameters themselves may become unphysical. In this section the best way of fitting phase differences and amplitude ratios is examined.

There are four physically reasonable ways of fitting the phase difference: While the k^1 term must always be retained, the k^{-1} and k^3 terms can or cannot be discarded, which allows determination of the following combinations of parameters:

(P1) ΔR,

(P2) ΔE, ΔR,

(P3) ΔR, $\Delta\sigma^{(3)}$,

(P4) ΔE, ΔR, $\Delta\sigma^{(3)}$.

Similarly, the amplitude ratio must always contain the k^2 term whereas the k^0 and k^4 terms are not mandatory, giving rise to four possibilities:

(A1) $\Delta\sigma^2$,
(A2) $\Delta\lambda$, $\Delta\sigma^2$,
(A3) $\Delta\sigma^2$, $\Delta\sigma^{(4)}$,
(A4) $\Delta\lambda$, $\Delta\sigma^2$, $\Delta\sigma^{(4)}$.

We choose $\Delta\lambda$ rather than ΔN since the coordination number definitely remains constant under high pressure.

The ΔR results are immediately coverted into pressures using the Murnaghan equation of state[33]

$$p=\frac{B_0}{B_0'}\left[\left[\frac{R_0}{R_0-\Delta R}\right]^{3B_0'}-1\right], \tag{11}$$

where R_0 is the nearest-neighbor distance at zero pressure and B_0 and B_0' denote the bulk modulus and its first pressure derivative at zero pressure. B_0 (141.5 GPa) and B_0' (4.36) were determined from fitting (11) to the copper compression values of the AIP handbook[34] in the range 0–20 GPa. This fit is excellent, incurrring virtually no error. When (11), with the same values for B_0 and B_0', is superimposed on the compression values of Vaidya and Kennedy[35] and Xu *et al.*[36] systematic deviations of up to 0.2 GPa at 4.5 GPa and 0.6 GPa at 8.4 GPa, respectively, occur. So the possibility of a systematic error of up to 0.7 GPa at 10.0 GPa exists. We do not want to investigate this problem further since it is not related to EXAFS and not limited to copper. It is rather a problem of all high-pressure work.

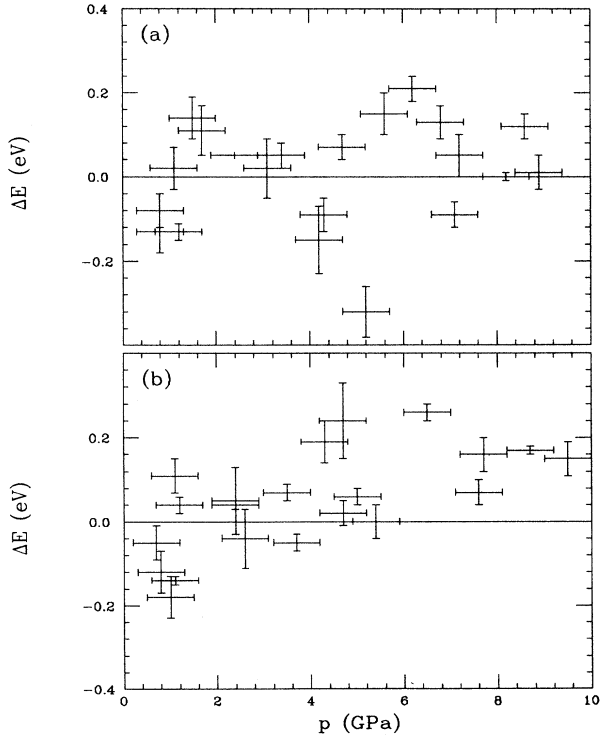

FIG. 2. Energy shift $\Delta E(p)$ calculated (a) with method (P2) and (b) with method (P4).

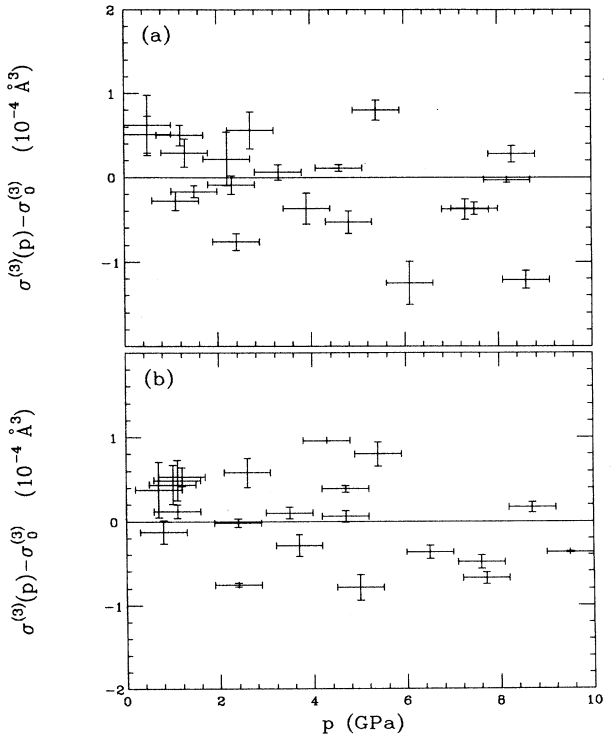

FIG. 3. Change in third cumulant $\sigma^{(3)}(p)-\sigma_0^{(3)}$ calculated (a) with method (P3) and (b) with method (P4).

After having converted ΔR to pressure,

$$\Delta E(p)\ ,$$
$$-\Delta\sigma^{(3)}(p)=\sigma^{(3)}(p)-\sigma_0^{(3)}\ ,$$
$$-\Delta\sigma^2(p)=\sigma^2(p)-\sigma_0^2\ ,$$
$$-\Delta\lambda(p)=\lambda(p)-\lambda_0\ ,$$
$$-\Delta\sigma^{(4)}(p)=\sigma^{(4)}(p)-\sigma_0^{(4)}$$

are shown in Figs. 2–6. Of the 42 results only one-half (with the smallest goodness-of-fit parameters) are plotted.

Figure 2 shows $\Delta E(p)$, calculated with methods (P2) and (P4). It is evident that the variations are random, except for a slight increase with pressure of $\Delta E(p)$ by about (0.15 eV)/(10 GPa) with method (P4). Figure 3 shows that $\sigma^{(3)}(p)-\sigma_0^{(3)}$, calculated with both methods (P3) and (P4), is independent of pressure and exhibits only random fluctuations. The random fluctuations are a result of the strong correlations between the pairs of parameters $R\leftrightarrow\Delta E$ and $R\leftrightarrow\sigma^{(3)}$.

The parameter-fitting routine can be used to calculate the goodness-of-fit parameter of a simulated EXAFS set with all parameters kept constant. When this is done repeatedly with slightly wrong values for R and ΔE, or R and $\sigma^{(3)}$, a two-dimensional array of goodness-of-fit parameters (parameter space) is created. The topography of the parameter space $R\leftrightarrow\Delta E$ has a valley with almost identical goodness-of-fit parameters from R (=2.554 Å)/ΔE (=−0.4 eV) to R (=2.562 Å)/

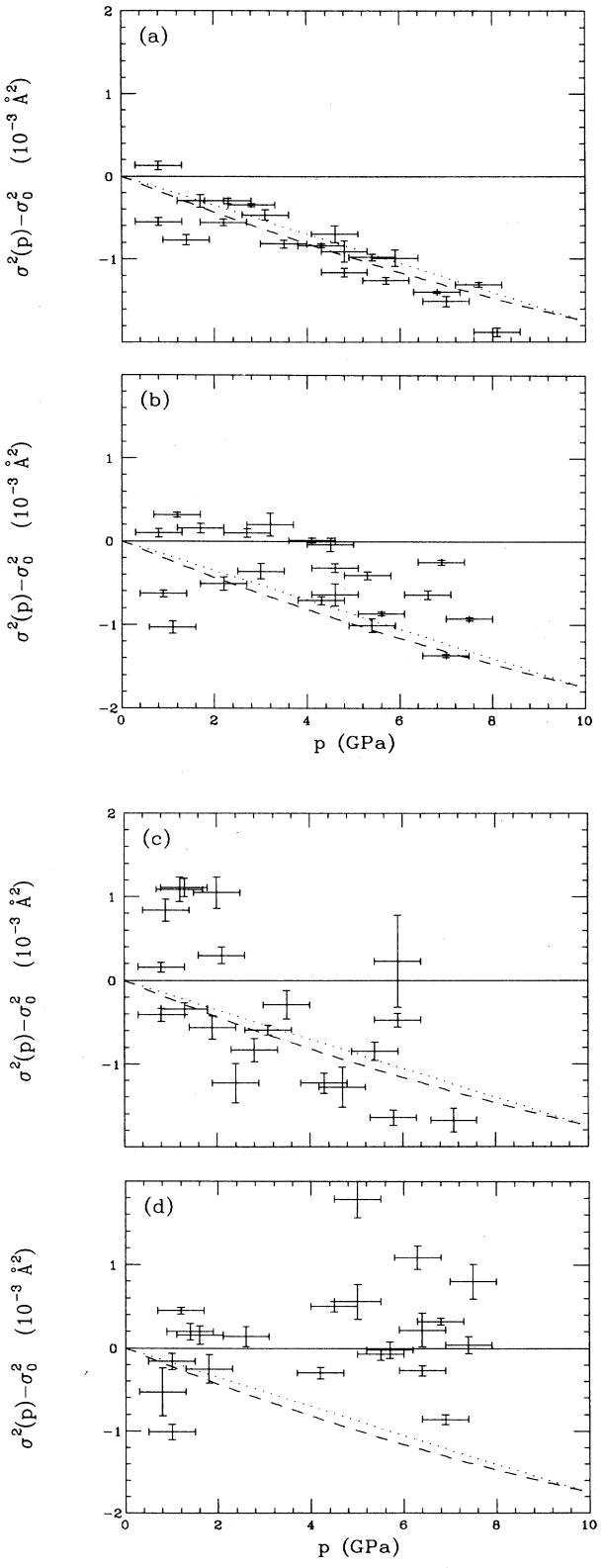

FIG. 4. Change in second cumulant (EXAFS Debye-Waller factor) $\sigma^2(p)-\sigma_0^2$ calculated (a) with method (A1), (b) with method (A2), (c) with method (A3), and (d) with method (A4). The dashed and dotted curves are $\sigma^2(p)-\sigma_0^2$ as calculated from Eq. (16) and Eqs. (18a), (19), and (21), respectively.

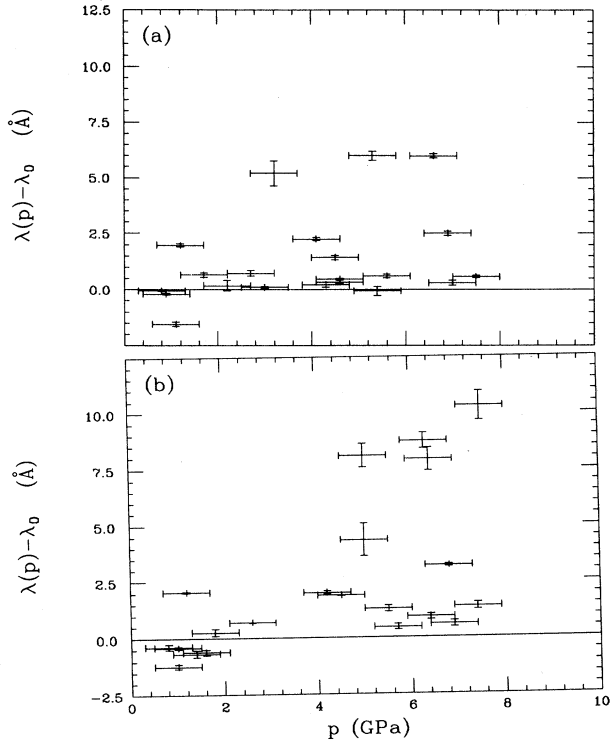

FIG. 5. Change in the λ parameter $\lambda(p)-\lambda_0$ calculated (a) with method (A2) and (b) with method (A4).

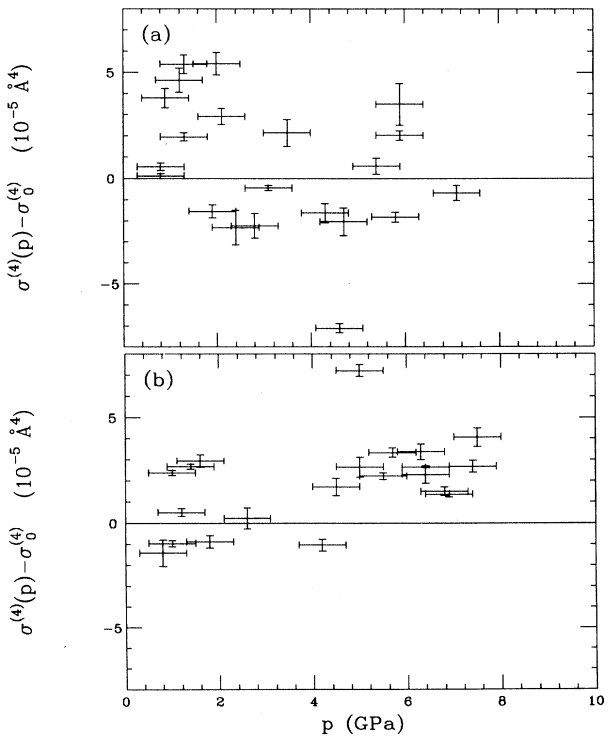

FIG. 6. Change in fourth cumulant $\sigma^{(4)}(p)-\sigma_0^{(4)}$ calculated (a) with method (A3) and (b) with method (A4).

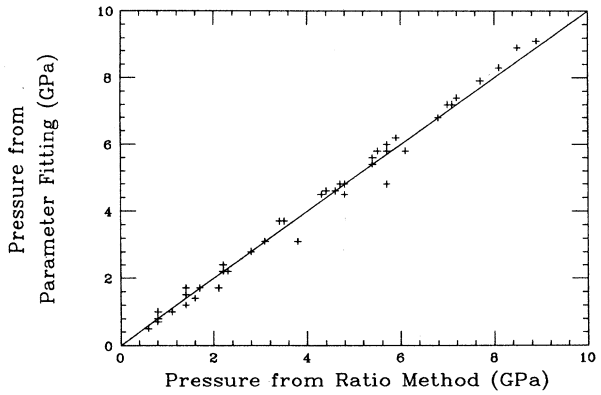

FIG. 7. Pressures determined from the ratio method and from parameter fitting.

ΔE (=1.0 eV), indicating that R and ΔE are interchangeable with a ratio of (0.006 Å)/(1 eV). Similarly, R and $\sigma^{(3)}$ are interchangeable with a ratio of 0.004 Å/10^{-4} Å^3 over a range of at least 0.008 Å/2.0×10^{-4} Å^3. Random oscillations of the order of 0.1 eV and 0.5×10^{-4} Å^3, respectively, can therefore easily be explained by the interchangeability of the three phase parameters. Should ΔE actually increase with pressure, as suggested by method (P4), then the neglect of this pressure dependence would result in an error of only 0.001 Å, or 0.2 GPa, at 10 GPa.

Thus, we conclude that both ΔE and $\sigma^{(3)}$ are physically independent of pressure and, in order to avoid a spurious scatter, method (P1) is a legitimate way of determining ΔR in copper. This lucky circumstance makes copper an ideal pressure marker in high-pressure EXAFS experiments. It must be borne in mind that the legitimacy of this simplification has been demonstrated *only for copper*. In general, pressure-induced energy shifts and changes in third cumulants must be taken into account until they have been proven to be negligible. Neglecting them right from the beginning of data analysis could result in serious errors in ΔR, as can be seen from the correlations mentioned before.

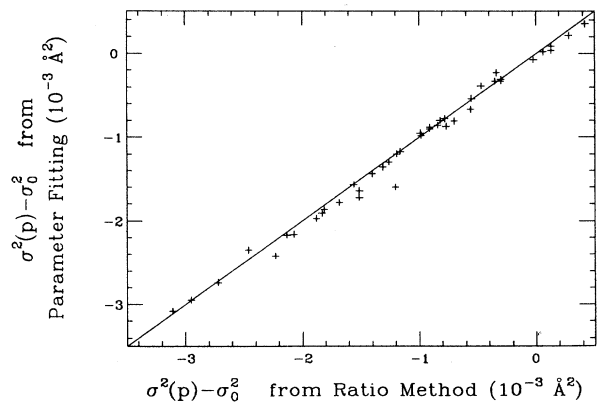

FIG. 8. Changes in the EXAFS Debye-Waller factor determined from the ratio method and from parameter fitting.

Figure 4 shows $\sigma^2(p)-\sigma_0^2$, calculated with methods (A1)–(A4). The dashed and the dotted lines indicate two completely independent theoretical calculations for the pressure dependence of the EXAFS Debye-Waller factor which are discussed in detail in the next section. It is clear both from the theories and from the small scatter of the data points that method (A1) is best, and that methods (A2)–(A4) must be discarded. There are two reasons why only one amplitude parameter can be retained. The amplitude, as opposed to the phase, is affected by various inaccuracies in the experiment and the data analysis, as explained before. Furthermore, the amplitude parameters are also strongly intercorrelated: σ^2 and λ are almost interchangeable with a ratio of 0.8×10^{-3} Å^2/(1 Å) over a range of about 0.7×10^{-3} Å/0.9 Å. Similarly, σ^2 and $\sigma^{(4)}$ are interchangeable with 0.2×10^{-3} Å^2/10^{-5} Å^4 over a range of 1.1×10^{-3} Å/5.0×10^{-5} Å^4.

In choosing method (A1) we are, therefore, asserting that both λ and $\sigma^{(4)}$ have negligible pressure dependence and that the variations seen in Figs. 5 and 6 are spurious and a result of these correlations. While for λ such a behavior seems physically reasonable, no predictions can be made regarding the fourth cumulant. But it must be borne in mind that σ^2 and $\sigma^{(4)}$ are unequal quantities because they are second- and fourth-order terms, respectively. Neglect of $\sigma^{(4)}$ should therefore have little consequences for the other amplitude parameters. Noting that $\sigma^{(4)}$ could not even be determined reliably from simulated EXAFS data we are not surprised to find it nothing but a source of error in real-data analysis.

Figure 7 presents a comparison between the pressures determined from the ratio method and from parameter fitting. To make the results comparable, method (P1) was applied in the ratio program, and R was the only phase parameter fitted in the parameter-fitting routine. Figure 7 demonstrates convincingly that both techniques yield basically the same results, i.e., that the theoretical phases $\Phi(k)$ and amplitudes $F(k,\pi)$ use in parameter fitting are reliable and that the errors inherent in the ratio- and parameter-fitting techniques are only about 0.2 GPa. It must be mentioned here that no use was made of the slight variation with nearest-neighbor distance of McKale's backscatter amplitude and phase. Therefore, this makes parameter fitting comparable to the ratio method which is based on the assumption of identity of $\Phi(k)$ and $F(k,\pi)$ in both data sets. When McKale's functions are made nearest-neighbor-distance dependent (which requires an iterative fitting procedure) the pressures increase by about 0.2 GPa at 10 GPa. We do not make use of this possibility which would render the ratio technique obsolete and make us rely entirely on parameter fitting.

Figure 8 shows a comparison between $\Delta\sigma^2$ determined from the ratio program and from parameter fitting. Method (A1) was used in the ratio program and σ^2 was the only amplitude parameter fitted. Again the results are very much alike. Use of McKale's nearest-neighbor-distance dependence of the backscatter amplitude has only negligible influence on the fitting of σ^2. All 42 data

points were plotted in Figs. 7 and 8, irrespective of the goodness-of-fit parameters.

Another type of parameter fitting was also attempted where phases and amplitudes were extracted from the zero-pressure data sets and used to fit the high-pressure sets. This procedure yields results even more similar to the ones from the ratio technique.

VII. DISCUSSION OF σ^2

Figure 4 contains graphs obtained from two independent theoretical calculations of the EXAFS Debye-Waller factor as a function of pressure. The first approach starts with the definition of the mode-dependent Grüneisen parameter γ_ω,

$$\gamma_\omega = -\frac{\partial \ln\omega}{\partial \ln V} . \tag{12a}$$

In Debye theory all frequencies are just fractions of the Debye frequency ω_D, thus

$$\gamma_\omega = \gamma = -\frac{\partial \ln\omega_D}{\partial \ln V} . \tag{12b}$$

This mode-independent Grüneisen parameter still depends on volume which, in turn, depends on pressure. With a slight modification of a formula found in the literature[37,38] the simplest parametrization of the volume dependence for copper can be written as

$$\frac{\gamma(V(p))}{V(p)} = \frac{\gamma(V_0)}{V_0} = \text{const} , \tag{13}$$

where the subscript 0 indicates zero pressure. Following the literature[38–41] $\gamma(V_0)$ is taken to be 2.0. Integration of (12b) gives

$$\omega_D(V(p)) = \omega_D(V_0)\exp\left[\gamma(V_0)\left[1-\frac{V(p)}{V_0}\right]\right] . \tag{14}$$

$\omega_D(V_0)$ is related to the Debye temperature, $\Theta_D(V_0)$, by $\hbar\omega_D = k_B\Theta_D$. $\Theta_D(V_0)$ is 315 K.[42] For $[V(p)/V_0]$ any appropriate isothermal equation of state can be used, e.g.,[43]

$$\frac{V(p)}{V_0} = \left[1-\frac{1}{3B_0'+1}\ln\left[1+\frac{3B_0'+1}{3B_0}p\right]\right]^3 . \tag{15}$$

Equation (14) together with (15) is then inserted into a correlated Debye model calculation which expresses the EXAFS Debye-Waller factor as a function of the Debye frequency[6]

$$\sigma^2(p) = \frac{3\hbar}{M\omega_D^3(p)}\int_0^{\omega_D(p)}\omega\left[1-\frac{\sin\left[C\frac{\omega}{\omega_D(p)}\right]}{C\frac{\omega}{\omega_D(p)}}\right] \times\coth\left[\frac{\hbar\omega}{2k_BT}\right]d\omega \tag{16a}$$

with

$$C = \frac{(6\pi^2\rho_0)^{1/3}R_0}{M^{1/3}} \tag{16b}$$

where ρ_0 and M are the density at zero pressure and the atomic mass, respectively.

The second approach starts from the definition of the cumulants in terms of moments, i.e., Eq. (3). The nth moment μ_n is defined by

$$\mu_n(p) = \frac{\sum_i r_i^n e^{-\Delta S_i(p)/k_B}}{\sum_i e^{-\Delta S_i(p)/k_B}} . \tag{17a}$$

r_i denotes the momentary distance to the nearest neighbor as before. $\Delta S_i(p)$ is the difference between the ground-state entropy and the entropy of a given state, i. Pressure p is a parameter. The summation is over all states. The system under investigation is one bond, i.e., $\frac{2}{12}$ of the Wigner-Seitz cell for copper. Replacing the summation by an integration over a six-dimensional phase space (the two-body problem becomes a one-body problem in c.m. coordinates) with three momentum variables $\mathbf{p}$ (not to be confused with pressure, p) and three spatial variables $\mathbf{q}$ gives

$$\mu_n(p) = \frac{\int\int r^n(\mathbf{q})e^{-\Delta S(p;\mathbf{p},\mathbf{q})/k_B}\,d\mathbf{p}\,d\mathbf{q}}{\int\int e^{-\Delta S(p;\mathbf{p},\mathbf{q})/k_B}\,d\mathbf{p}\,d\mathbf{q}} . \tag{17b}$$

The first law relates $\Delta S(p;\mathbf{p},\mathbf{q})$ to volume $\Delta V(\mathbf{q})$, potential energy $\Delta E_p(\mathbf{q})$, and kinetic energy $\Delta E_k(\mathbf{p})$ by

$$\Delta S(p;\mathbf{p},\mathbf{q}) = \frac{1}{T}[p\,\Delta V(\mathbf{q}) + \Delta E_p(\mathbf{q}) + \Delta E_k(\mathbf{p})] .$$

Obviously, the integration over $\mathbf{p}$ cancels and $\mathbf{q}$ can be replaced by r in this one-dimensional problem. Writing $x = r - R'$, where R' is the minimum of the potential energy (not to be confused with the average nearest-neighbor distance at zero pressure R_0), expanding the changes in volume and potential energy in powers of x and retaining only first-order terms in $\Delta V(x)$ (not valid for very large p) and third-order terms in $\Delta E_p(x)$, one arrives at

$$\mu_n(p) = \frac{\int (R'+x)^n e^{-(apx+bx^2-cx^3)/k_BT}\,dx}{\int e^{-(apx+bx^2-cx^3)/k_BT}\,dx} , \tag{17c}$$

where a,b,c are positive, and so far unknown, parameters.

The preceding ansatz that isolates one single bond and neglects all others is based on four assumptions. (1) Equation (17c) is a classical average and works only for temperatures greater than about $\frac{1}{2}\Theta_D$. This poses no problem in our investigation. (2) Possible interactions with higher shells are neglected. This is a good approximation for copper.[44,45] (3) The ansatz is strictly applicable only if all bond angles are right angles. Then the displacement of one bond is, to first order in x, independent

of the displacement of all other bonds. Since in copper there are 90° and 60° bond angles errors may be expected. (4) The anharmonic terms in a Taylor expansion of the potential energy generally contain multibody potentials, i.e., three-body potentials for the third-order term, etc. Moriarty[46,47] has shown from first principles that three-body potentials are negligible in copper. Since nothing is known about four-body potentials the potential energy expansion must be terminated after the cubic term which could result in a further deterioration of the results.

When the cubic term in (17c) is expanded to first order the equation can be integrated. With (3) one obtains

$$\sigma^{(1)}(p)=R'+\frac{3(k_BT)c}{4b^2}-\frac{1}{2b}(ap)+\frac{3c}{8b^3}(ap)^2 , \tag{18a}$$

$$\sigma^2(p)=\frac{(k_BT)}{2b}-\frac{3(k_BT)c}{4b^3}(ap) . \tag{18b}$$

Since $\sigma^{(1)}(p)=\mu_1(p)=R(p)$,

$$\sigma_0^{(1)}=R_0 \text{ and } R_0=R'+\frac{3(k_BT)c}{4b^2} .$$

Equations (18) have the interesting property

$$\sigma^2(p)=(-k_BT)\frac{d\sigma^{(1)}(p)}{d(ap)} . \tag{19}$$

The parameter a can be determined from (19) by noting that

$$-\frac{dp}{B(p)}=\frac{dV(p)}{V(p)}=\frac{3\,dR(p)}{R(p)}=\frac{3\,d\sigma^{(1)}(p)}{R(p)} \tag{20}$$

giving

$$a=\frac{(k_BT)R_0}{3B_0\sigma_0^2} . \tag{21}$$

σ_0^2 must be taken from the literature. The problem is thus reduced to getting an appropriate formulation for $\sigma^{(1)}(p)$. Noting that

$$\frac{\sigma^{(1)}(p)}{R_0}=\left[\frac{V(p)}{V_0}\right]^{1/3} , \tag{22}$$

the parameters b and c can be obtained from fitting (18a) to compression data, $[V(p)/V_0]$, from the literature.

Figure 4 contains plots of $-\Delta\sigma^2(p)=\sigma^2(p)-\sigma_0^2$ from the two theories just presented. They are in good agreement with each other and with the data. From (18b) one sees that $\Delta\sigma^2(p)$ is a third-order term, determined by a third-order coefficient c. It seems that high-pressure EXAFS contains information on third-order elastic constants (TOEC). Further investigations are called for.

Everything that has been said cumulants so far refers to *thermal cumulants,* i.e., those cumulants that result from the thermal motion of the atoms. We must now examine the possibility of *static cumulants* which result from a static disorder of the atoms. Neglecting the disorder due to point defects and along dislocations and grain boundaries, there is one possibility for static cumulants in copper under high pressure: The pressure inside the sample is possibly nonhydrostatic or inhomogeneous. To estimate this effect we assume that the variation of pressure inside the sample can be approximated by a parabola

$$p(x)=p_{\max}\left[1-\frac{x^2}{\rho^2}\right] , \tag{23}$$

where x is the radial distance from the center of the sample, ρ is the radius of the anvil flat, and $p_{\max}$ is the pressure at the center of the sample which is $\frac{18}{17}$ of the pressure averaged over the sample if the sample diameter is $\frac{1}{3}$ of the anvil flat diameter. It can be shown in a straightforward calculation that, to first order, the nearest-neighbor distance is also given by a parabola

$$R(x)=a+b\frac{x^2}{\rho^2} , \tag{24}$$

where a and b are constants that depend on the average pressure. From the distribution (24) moments and cumulants can be calculated in the same fashion as before. The results are $\sigma^2=2.4\times10^{-6}$ Å^2 and $\sigma^{(3)}=0$ at $p=10$ GPa. Pressure inhomogeneity is therefore no possible source of error in the preceding calculation.

We want to conclude this section by mentioning that a similar investigation of the pressure dependence of the EXAFS Debye-Waller factor has come to our attention.[48] Unfortunately, no calculational details were given.

VIII. CONCLUSION

Bragg reflections in the diamond anvils of our high-pressure cell have produced serious interference with the EXAFS signal. The diamonds were replaced by boron-carbide anvils which are polycrystalline but, at the same time, intransparent for light, so the ruby-fluorescence pressure calibration had to be replaced. We have shown in great detail that the EXAFS of a copper foil put on top of the sample provides not only a reasonable but a very good replacement for the rubies. We have also shown that the EXAFS amplitude, even though it is less reliable than the phase, contains useful information.

We now summarize the errors in the determination of pressure from the EXAFS phase. (1) The Fourier back-transform from **r** space to **k** space produces an error of about 0.001 Å, or 0.2 GPa, which must be taken into account. (2) The ratio- and parameter-fitting programs give results that differ by about 0.2 GPa. This is the intrinsic error of the routines and must be taken into account. (3) Neglect of the nearest-neighbor-distance dependence of the backscattering phase may introduce an error ranging from 0.0 GPa (at 0 GPa) to 0.2 GPa (at 10 GPa). If this nearest-neighbor-distance dependence is acknowledged as correct the ratio technique becomes obsolete. We rather chose to keep the ratio method and incur this possible extra error. (4) There is the remote possibility that ΔE does depend on pressure and its neglect introduces an error of 0.2 GPa (at 10 GPa).

We take errors (1)–(3) into account and conclude that the overall error in pressure determination is about 0.5 GPa. The ruby-fluorescence pressure calibration,[49] in

comparison, supposedly produces errors from about 0.1 GPa (at 1 GPa) to about 0.8 GPa (at 20 GPa), i.e., about 0.1–0.4 GPa in our range of interest. In addition to that, there is the possibility that we calibrate the pressures with a wrong scale. This is not EXAFS-related or a special feature of copper but common to all high-pressure work.

ACKNOWLEDGMENTS

We would like to thank N. Alberding, A. J. Seary, and K. R. Bauchspiess, our collaborators from Simon Fraser University, and J. M. Tranquada, J. E. Whitmore, and B. Houser, our University of Washington group, for having done the experiments with us at SSRL. We would also like to thank J. M. Brown and J. J. Rehr for valuable discussions. This work was supported by the U.S. Department of Energy Grant Nos. DE-AT06-83ER45038 and DE-FG06-84ER45163, and by the National Science and Engineering Research Council of Canada. SSRL is supported by the U.S. Department of Energy (Office of Basic Energy Sciences) and the National Institutes of Health (Biotechnology Research Program, Division of Research Resources).

[1]O. Shimomura *et al.*, in *High Pressure Science and Technology,* edited by B. Vodar and Ph. Marteau (Pergamon, Oxford, 1980), p. 534.
[2]R. Ingalls *et al.*, J. Appl. Phys. **51**, 3158 (1980).
[3]R. Ingalls, J. M. Tranquada, J. E. Whitmore, and E. D. Crozier, in *Physics of Solids under High Pressure,* edited by J. S. Schilling and R. N. Shelton (North-Holland, Amsterdam, 1981), p. 67.
[4]J. M. Tranquada and R. Ingalls, in *EXAFS and Near Edge Structure III,* edited by K.O. Hodgson, B. Hedman, and J. E. Penner-Hahn (Springer-Verlag, Berlin, 1984), p. 388.
[5]J. M. Tranquada and R. Ingalls, Phys. Rev. B **34**, 4267 (1986).
[6]E. Sevillano, H. Meuth, and J. J. Rehr, Phys. Rev. B **20**, 4908 (1979).
[7]T. M. Hayes and J. B. Boyce, Solid State Phys. **37**, 173 (1982).
[8]J. M. Tranquada and R. Ingalls, Phys. Rev. B **28**, 3520 (1983).
[9]E. A. Stern and K. Kim, Phys. Rev. B **23**, 3781 (1981).
[10]J. Goulon, C. Goulon-Ginet, R. Cortes, and J. M. Dubois, J. Phys. (Paris) **43**, 539 (1982).
[11]J. J. Boland, F. G. Halaka, and J. D. Baldeschwieler, Phys. Rev. B **28**, 2921 (1983).
[12]B.-K. Teo, in *EXAFS Spectroscopy: Techniques and Applications,* edited by B.-K. Teo and D. C. Joy (Plenum, New York, 1981), p. 31.
[13]J. Tranquada, Ph.D. thesis, University of Washington, Seattle, 1983.
[14]E. D. Crozier, J. J. Rehr, and R. Ingalls, in *X-Ray Absorption,* edited by D. C. Koningsberger and R. Prins (Wiley, New York, 1988), p. 373.
[15]M. G. Kendall, *The Advanced Theory of Statistics* (Griffin, London, 1948), Vol. I, pp. 60–64.
[16]E. A. Stern, D. E. Sayers, and F. Lytle, Phys. Rev. B **11**, 4836 (1975).
[17]G. Bunker, Nucl. Instrum. Methods **207**, 437 (1983)
[18]P. A. Lee, P. H. Citrin, P. Eisenberger, and B. M. Kincaid, Rev. Mod. Phys. **53**, 769 (1981).
[19]S. J. Gurman and J. B. Pendry, Solid State Commun. **20**, 287 (1976).
[20]W. Böhmer and P. Rabe, J. Phys. C. **12**, 2465 (1979).
[21]R. B. Greegor and F. W. Lytle, Phys. Rev. B **20**, 4902 (1979).
[22]B. Lengeler and P. Eisenberger, Phys. Rev. B **21**, 4507 (1980).
[23]E. A. Stern, B. A. Bunker, and S. M. Heald, Phys. Rev. B **21**, 5521 (1980).
[24]B.-K. Teo and P. A. Lee, J. Am. Chem. Soc. **101**, 2815 (1979).
[25]P. A. Lee, B. K. Teo, and A. L. Simons, J. Am. Chem. Soc. **99**, 3856 (1977).
[26]A. G. McKale *et al.*, J. Phys. (Paris) Colloq., Suppl. 12 **47**, C8-55 (1986).
[27]A. G. McKale, G. S. Knapp, and S.-K. Chan, Phys. Rev. B **33**, 841 (1986).
[28]A. G. McKale *et al.*, J. Am. Chem. Soc. **110**, 3763 (1988).
[29]Ph. R. Bevington, *Data Reduction and Error Analysis for the Physical Sciences* (McGraw-Hill, New York, 1969), p. 204.
[30]W. H. Press, B. P. Flannery, S. A. Teukolsky, and W. T. Vetterling, *Numerical Recipes* (Cambridge University Press, Cambridge, 1986), p. 274.
[31]D. E. Sayers and B. A. Bunker, in Ref. 14, p. 211.
[32]J. W. Cook and D. E. Sayers, J. Appl. Phys. **52**, 5024 (1981).
[33]F. D. Murnaghan, Proc. Nat. Acad. Sci. U.S.A. **30**, 244 (1944).
[34]*American Institute of Physics Handbook,* 3rd ed. (AIP, New York, 1972), pp. 4–100.
[35]S. N. Vaidya and G. C. Kennedy, J. Phys. Chem. Solids **31**, 2329 (1970).
[36]J. Xu, H.-K. Mao, and P. M. Bell, High Temp.—High Pressures **16**, 495 (1984).
[37]J. Ramakrishnan, R. Boehler, G. H. Higgins, and G. C. Kennedy, J. Geophys. Res. **83**, 3535 (1978).
[38]U. Walzer, W. Ullmann, and V. L. Pan'kov, Phys. Earth Planet. Inter. **18**, 1 (1979).
[39]H. L. Kharoo, O. P. Gupta, and M. P. Hemkar, J. Phys. Chem. Solids **39**, 45 (1978).
[40]M. Delannoy and G. Perrin, J. Phys. Solids **41**, 11 (1980).
[41]O. P. Gupta and H. L. Kharoo, J. Chem. Phys. **74**, 3577 (1981).
[42]N. W. Ashcroft and N. D. Mermin, *Solid State Physics* (Holt, Rinehart and Winston, New York, 1976).
[43]J. Freund and R. Ingalls, J. Phys. Chem. Solids **50**, 263 (1989).
[44]R. M. Nicklow *et al.*, Phys. Rev. **164**, 922 (1967).
[45]E. C. Svensson, B. N. Brockhouse, and J. M. Rowe, Phys. Rev. **155**, 619 (1967).
[46]J. A. Moriarty, Phys. Rev. Lett. **55**, 1502 (1985).
[47]J. A. Moriarty, in *Shock Waves in Condensed Matter,* edited by Y. M. Gupta (Plenum, New York, 1986), p. 101.
[48]A. Polian *et al.*, Phys. Rev. B **39**, 3369 (1989).
[49]G. J. Piermarini, S. Block, J. D. Barnett, and R. A. Forman, J. Appl. Phys. **46**, 2774 (1975).